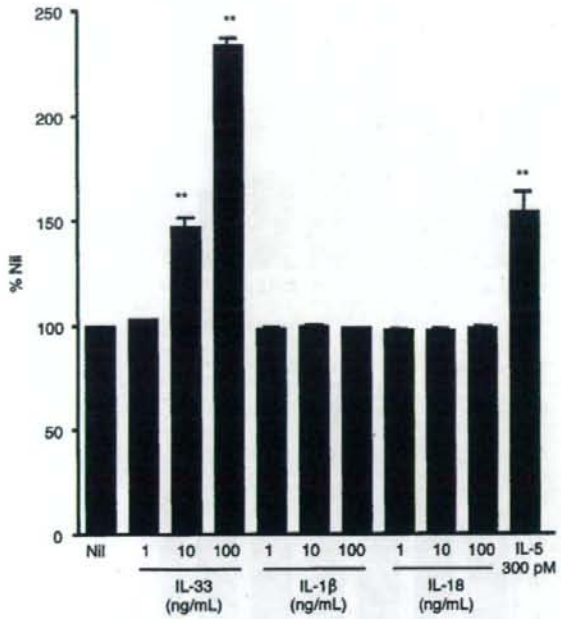

Figure 3 The effect of IL-33 on eosinophil CD11b expression. Human eosinophils were incubated with the indicated reagent for 30 min, and then the cell-surface expression of CD11b was analyzed by flow cytometry. The data are expressed as the percentage of the calculated MESF values of eosinophils cultured without stimulus (% nil). Bars represent the s.e.m. ($n=3$). $^{**}P<0.01$ *vs* nil.

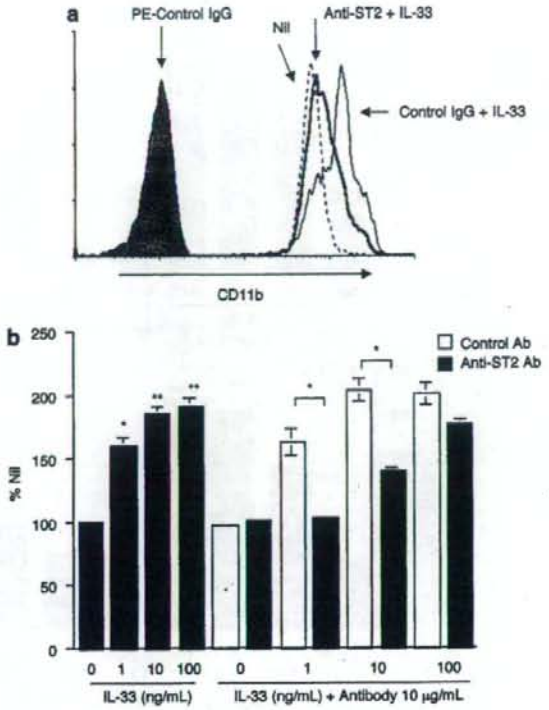

Figure 4 The effect of anti-ST2 neutralizing antibody on CD11b expression by eosinophils. **(a)** Human eosinophils were preincubated with anti-ST2 antibody at 10 μg/ml for 60 min and then with IL-33 at 10 ng/ml for 30 min. The surface CD11b expression level was assessed by flow cytometry. Eosinophils stained with PE-control mouse IgG1 are shown as a shaded area. Data are representative of four separate experiments showing similar results. **(b)** Human eosinophils were preincubated with or without anti-ST2 antibody or control antibody at 10 μg/ml for 60 min and then with IL-33 at the indicated concentrations for 30 min. The data are expressed as the percentage of the calculated MESF values of eosinophils cultured without antibodies or stimulus (% nil). Bars represent the s.e.m. ($n=3$). $^{*}P<0.05$, $^{**}P<0.01$ *vs* nil.

To elucidate the role of ST2 in eosinophil survival, neutralizing antibody for ST2 was added together with IL-33. As a result, anti-ST2 antibody at 20 μg/ml significantly downmodulated the effect of IL-33, as shown by a decreased number of live cells and an increased number of apoptotic cells (Figure 6a and b), indicating that IL-33 enhances eosinophil survival by signaling through the ST2 receptor.

It has been reported that eosinophils can produce IL-5 upon stimulation. We used neutralizing antibody for IL-5 to test the possibility that IL-33 enhancement of eosinophil survival was mediated by IL-5. However, anti-IL-5 antibody did not affect the number of viable eosinophils cultured with IL-33 (data not shown). Similar tests using anti-IL-4 and anti-GM-CSF neutralizing antibody gave the same result. These results indicate that the effect of IL-33 on eosinophil survival is not mediated by autocrine activation involving IL-5, IL-4 or GM-CSF.

Analysis of Degranulation and Lipid Mediator Synthesis

We conducted experiments to see whether IL-33 induces degranulation and lipid mediator synthesis in human eosinophils. Eosinophil degranulation was analyzed by measuring EDN, but IL-33 was negative for this activity (data not shown). LTC4 synthesis was analyzed by ELISA, but no apparent release of LTC4 was induced by IL-33 (data not shown).

DISCUSSION

In the present study, we assessed the potential role of IL-33 in regulation of eosinophil functions. We demonstrated that IL-33 is a potent activator of human eosinophils, enhancing their surface CD11b expression and adhesion and prolonging their life span. Surprisingly, the maximal enhancing effects of IL-33 on adhesion and CD11b expression were comparable to, or even greater than, the effects of IL-5, a potent eosinophil-activating cytokine. This is the first report showing direct effects of IL-33 on the biological functions of eosinophils. Importantly, the effects of IL-33 on eosinophils were limited to cell adhesion and survival, in clear contrast to

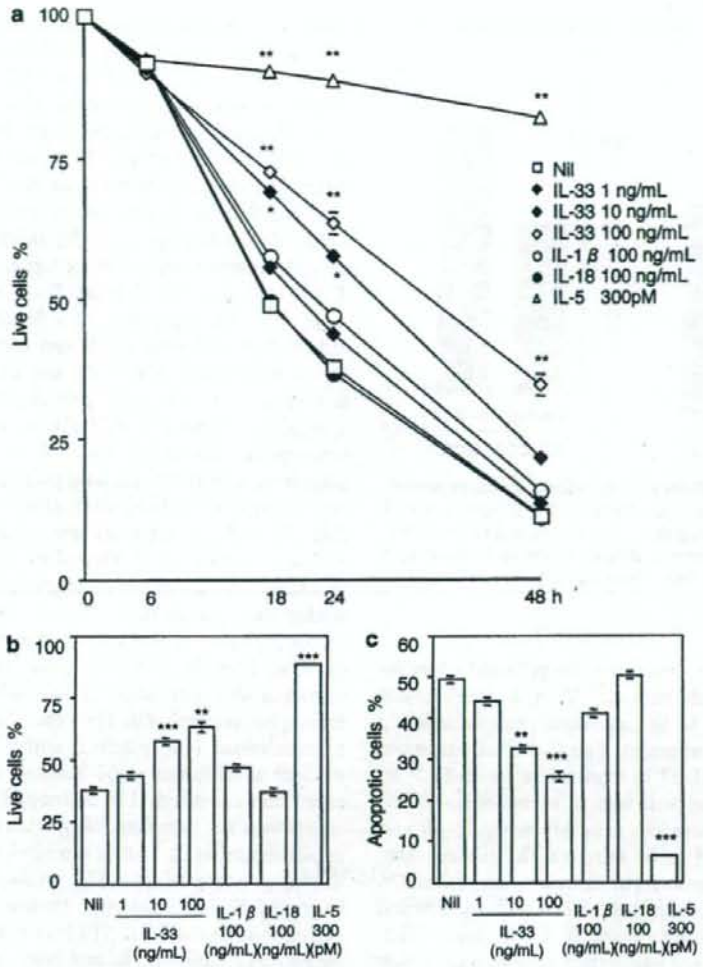

Figure 5 IL-33 enhances survival of eosinophils. (**a**) Time course of survival of human eosinophils. Highly purified eosinophils were cultured in medium alone or in the presence of IL-33 (1, 10 and 100 ng/ml), IL-1β (100 ng/ml), IL-18 (100 ng/ml) or IL-5 (300 pM) for the indicated times. The cells were analyzed by double staining with annexin V and PI. Live cells were negative for both annexin V and PI. Data are expressed as percentages of total cell numbers. (**b**, **c**) Viable (**b**) and apoptotic eosinophils (**c**) after 24-h incubation. Early apoptotic cells were defined as annexin V-positive and PI-negative. Bars represent the s.e.m. ($n=4$). $^{*}P<0.05$, $^{**}P<0.01$ and $^{***}P<0.001$ *vs* medium alone.

IL-5, which also affects mediator synthesis and release by eosinophils.[23,24]

IL-33 is a recently identified cytokine belonging to the IL-1 family. It has increasingly been thought that IL-33 may be involved in the pathogenesis of Th2-polarized inflammation. Schmitz *et al*[14] demonstrated that IL-33 induces Th2-polarized cells to produce Th2 cytokines such as IL-5 and IL-13. In addition, *in vivo* exposure to IL-33 causes histological changes in the lungs and gastrointestinal tract, including eosinophilic and mononuclear cell infiltration, increased mucus production, and epithelial cell hyperplasia and hypertrophy.[14] Although the principal source of IL-33 in Th2-related allergic diseases has yet to be determined, this cytokine can reportedly be produced by many cell types including epithelial cells and smooth muscle cells.[25] Thus, IL-33 secreted by various cell types may act collectively to induce allergic inflammation through Th2 cell differentiation and a direct effect on Th2 effector cells, including eosinophils.

Among the IL-1 family cytokines we tested, IL-33 was the only one that activated eosinophil functions. In previous studies, IL-18, another IL-1 family cytokine, has been demonstrated to induce IL-8 production by eosinophils and to enhance antigen-induced eosinophil recruitment in mouse airways.[26,27] IL-1β has also been reported to enhance

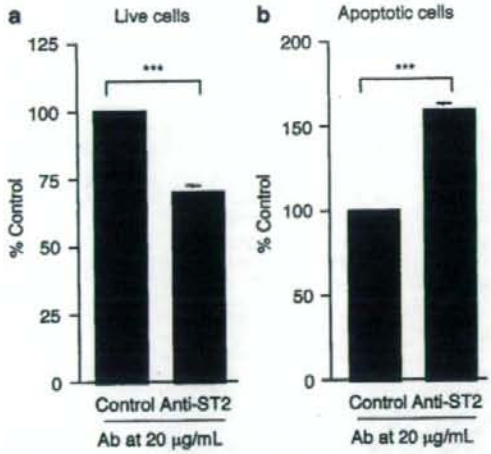

Figure 6 Effect of anti-ST2 antibody on IL-33-induced eosinophil survival. Highly purified eosinophils were cultured with IL-33 at 10 ng/ml and anti-ST2 neutralizing antibody at 20 μg/ml for 24 h. Live (**a**) and apoptotic (**b**) cells were analyzed by flow cytometry. Data are expressed as percentages of corresponding cells cultured with control antibody. Bars represent the s.e.m. ($n=5$). ***$P<0.001$ *vs* control.

mediator release from IgE-stimulated eosinophils and adhesiveness of eosinophils to endothelium.[28] Thus, the IL-1 family cytokines are considered to be important proinflammatory cytokines in allergic inflammation. The IL-1 family member most closely related to IL-33 is reported to be IL-18.[14] In clear contrast to IL-33, the main cellular source of IL-1β and IL-18 seems to be hematopoietic cells. Moreover, IL-1β and IL-18 are not considered to be selective Th2-related cytokines, as they can also promote Th1-associated responses. On the basis of our present study, IL-33 seems to have different roles from IL-1β and IL-18. Thus, IL-33 promotes Th2-associated responses, at least partly through direct activation of eosinophils, and this action seems unique among IL-1 family cytokines.

An IL-1 receptor family member, ST2, has been shown to function as an important effector molecule of Th2 responses in a number of experimental settings,[8,11] and it is an active receptor for IL-33. It has been demonstrated that expression of ST2 on Th2 cells is induced by proinflammatory substances, including TNF, IL-1α, IL-1β, IL-6, IL-5 and PMA, and importantly, crosslinking of ST2 provided a costimulatory signal for Th2 cells and directly induced Th2 cell proliferation and type 2 cytokine production.[29,30] Thus, ST2 might be important in the pathogenesis of diseases of the Th2 phenotype.

In the present study, real-time PCR analysis of eosinophils revealed that eosinophils express mRNA for ST2, although the expression level of mRNA was lower than that of mast cells which have already been reported to express ST2 on their cell surface.[10] Although surface expression of ST2 on eosinophils was hardly detectable, ST2 was shown to be present in the cells by intracellular flow cytometric analysis. At present, we do not know whether presumably faint levels of surface ST2 would suffice for triggering cell activation signals, or whether intracellular ST2 in eosinophils is also involved in cell activation by IL-33. However, based on the successful blocking of IL-33's effects by IL-33-neutralizing antibodies, we can reasonably say that ST2 protein expressed by eosinophils has functional relevance. In our present study, a high-affinity ST2 ligand, IL-33, induced a strong eosinophil adhesion response with efficacy higher than that of IL-5. The IL-1β, TNF-α, IFN-γ, IL-5 and IL-4 inflammatory cytokines upregulate the expression of adhesion molecules on the endothelium and eosinophils and increase eosinophil binding to endothelial cells.[31] On the basis of the findings of this study, IL-33, like other proinflammatory cytokines, also upregulated expression of CD11b, a component of Mac-1, on eosinophils. Therefore, the enhancement of eosinophil adhesiveness by IL-33 is at least partially due to this enhanced expression of CD11b. Neutralization experiments confirmed that β1 and β2 integrins are critically involved in the adhesion process of IL-33-treated eosinophils. Also, IL-33 prolonged the life span of eosinophils, although the effect was weaker than that of IL-5. We have shown that the survival-enhancing effect of IL-33 is not due to autocrine production of IL-4, IL-5 or GM-CSF, since neutralization of those cytokines did not affect IL-33-induced prolongation of eosinophil survival. On the other hand, at relatively high concentrations (10–20 μg/ml) anti-ST2 antibody was fairly efficient at inhibiting IL-33-induced upregulation of CD11b expression and survival of eosinophils, but those abrogating effects were not complete. We speculate that, in eosinophils, a small amount of IL-33 that can bind to cell-surface ST2 even in the presence of anti-ST2 antibody may act efficiently to modulate cell functions. Another possibility is that, in eosinophils, intracellular ST2 may not be completely blocked by anti-ST2 antibody. In any case, our results indicate that ST2 is an important receptor through which IL-33 mediates most, if not all, of various aspects of eosinophil activation.

Eosinophils are considered to be the most prominent cells at sites of allergic inflammation. Tissue eosinophils are believed to contribute to exacerbation of inflammation by an autocrine or paracrine mechanism. Therefore, marked reduction of tissue-infiltrated eosinophils is considered to be a promising therapeutic target for allergic diseases. On the basis of the findings of our present study, neutralization of ST2 abolished the effect of IL-33 on eosinophil activation indicating that IL-33 affected eosinophil function through ST2 although ST2 protein levels were low in eosinophils. In addition, in the clinical setting, elevated ST2 protein levels were reported in the sera of patients with asthma exacerbation, and the severity of asthma exacerbation correlated with the levels of serum ST2.[13] Furthermore, it has been demonstrated in a murine asthma model that administration of recombinant ST2 fusion protein attenuated eosinophilic inflammation of the airway and suppressed IL-4 and IL-5

production.[11] Thus, the IL-33–ST2 pathway may be actively involved in the pathogenesis of eosinophil-related allergic diseases such as asthma and eosinophilic gastroenteritis. In this context, several studies have shown that inhibition of the ST2-related signal pathway leads to abrogation of allergic diseases.[8,11,12]

In summary, we have explored for the first time the receptor expression and functions of IL-33 in human eosinophils, and we found that this cytokine potently activates eosinophils. In combination with previous reports by others, our results strongly suggest that the IL-33–ST2 pathway may be critically involved in the pathogenesis of allergic diseases. The effects of IL-33 on other inflammatory cells also need to be explored in detail; these information will help us understand the detailed mechanisms underlying clinical allergic diseases.

ACKNOWLEDGEMENTS

We thank Ms Chise Tamura for her skilled technical assistance and excellent secretarial work. Thanks are also extended to Ms Yasuko Asada for secretarial help, and Dr Koichi Hirai and Dr Toshiharu Nakajima for fruitful discussion on this manuscript. This work was supported by a grant from the Ministry of Education, Science, Sports and Culture of Japan, and grants-in-aid from the Ministry of Health, Labor and Welfare of Japan, and a Long-range Research Initiative (LRI) grant from the Japan Chemical Industry Association.

DISCLOSURE/DUALITY OF INTEREST

We have no duality of interest to declare.

1. Gleich GJ, Adolphson CR, Leiferman KM. The biology of the eosinophilic leukocyte. Annu Rev Med 1993;44:85–101.
2. Weller PF. The immunobiology of eosinophils. N Engl J Med 1991;324:1110–1118.
3. Lee T, Lenihan DJ, Malone B, *et al.* Increased biosynthesis of platelet-activating factor in activated human eosinophils. J Biol Chem 1984;259:5526–5530.
4. Klemenz R, Hoffmann S, Werenskiold AK. Serum- and oncoprotein-mediated induction of a gene with sequence similarity to the gene encoding carcinoembryonic antigen. Proc Natl Acad Sci USA 1989;86:5708–5712.
5. Tominaga S, Yokota T, Yanagisawa K, *et al.* Nucleotide sequence of a complementary DNA for human ST2. Biochim Biophys Acta 1992;1171:215–218.
6. Bergers G, Reikerstorfer A, Braselmann S, *et al.* Alternative promoter usage of the Fos-responsive gene Fit-1 generates mRNA isoforms coding for either secreted or membrane-bound proteins related to the IL-1 receptor. EMBO J 1994;13:1176–1188.
7. Yanagisawa K, Takagi T, Tsukamoto T, *et al.* Presence of a novel primary response gene ST2L, encoding a product highly similar to the interleukin 1 receptor type 1. FEBS Lett 1993;318:83–87.
8. Lohning M, Stroehmann A, Coyle AJ, *et al.* T1/ST2 is preferentially expressed on murine Th2 cells, independent of interleukin 4, interleukin 5, and interleukin 10, and important for Th2 effector function. Proc Natl Acad Sci USA 1998;95:6930–6935.
9. Lecart S, Lecointe N, Subramaniam A, *et al.* Activated, but not resting human Th2 cells, in contrast to Th1 and T regulatory cells, produce soluble ST2 and express low levels of ST2L at the cell surface. Eur J Immunol 2002;32:2979–2987.
10. Moritz DR, Rodewald HR, Gheyselinck J, *et al.* The IL-1 receptor-related T1 antigen is expressed on immature and mature mast cells and on fetal blood mast cell progenitors. J Immunol 1998;161:4866–4874.
11. Coyle AJ, Lloyd C, Tian J, *et al.* Crucial role of the interleukin 1 receptor family member T1/ST2 in T helper cell type 2-mediated lung mucosal immune responses. J Exp Med 1999;190:895–902.
12. Townsend MJ, Fallon PG, Matthews DJ, *et al.* T1/ST2-deficient mice demonstrate the importance of T1/ST2 in developing primary T helper cell type 2 responses. J Exp Med 2000;191:1069–1076.
13. Oshikawa K, Kuroiwa K, Tago K, *et al.* Elevated soluble ST2 protein levels in sera of patients with asthma with an acute exacerbation. Am J Respir Crit Care Med 2001;164:277–281.
14. Schmitz J, Owyang A, Oldham E, *et al.* IL-33, an interleukin-1-like cytokine that signals via the IL-1 receptor-related protein ST2 and induces T helper type 2-associated cytokines. Immunity 2005;23:479–490.
15. Iikura M, Suto H, Kajiwara N, *et al.* IL-33 can promote survival, adhesion and cytokine production in human mast cells. Lab Invest 2007;87:971–978.
16. Nagase H, Yamaguchi M, Jibiki S, *et al.* Eosinophil chemotaxis by chemokines: a study by a simple photometric assay. Allergy 1999;54:944–950.
17. Nakajima T, Inagaki N, Tanaka H, *et al.* Marked increase in CC chemokine gene expression in both human and mouse mast cell transcriptomes following FcεRI cross-linking: an interspecies comparison. Blood 2002;100:3861–3868.
18. Suzukawa M, Komiya A, Iikura M, *et al.* Trans-basement membrane migration of human basophils: role of matrix metalloproteinase-9. Int Immunol 2006;18:1575–1583.
19. Yoshimura C, Miyamasu M, Nagase H, *et al.* Glucocorticoids induce basophil apoptosis. J Allergy Clin Immunol 2001;108:215–220.
20. Fattah D, Page KR, Bezbaruah S, *et al.* A rapid activation assay for human eosinophils based on adhesion to immobilized ICAM-1, VCAM-1 and IgG. Cytokine 1996;8:248–259.
21. Suzukawa M, Hirai K, Iikura M, *et al.* IgE- and FcεRI-mediated migration of human basophils. Int Immunol 2005;17:1249–1255.
22. Yoshimura-Uchiyama C, Yamaguchi M, Nagase H, *et al.* Changing expression of IL-3 and IL-5 receptors in cultured human eosinophils. Biochem Biophys Res Commun 2003;309:26–31.
23. Takafuji S, Bischoff SC, de Weck AL, *et al.* IL-3 and IL-5 prime normal human eosinophils to produce leukotriene C4 in response to soluble agonists. J Immunol 1991;147:3855–3861.
24. Fujisawa T, Abu-Ghazaleh R, Kita H, *et al.* Regulatory effect of cytokines on eosinophil degranulation. J Immunol 1990;144:642–646.
25. Carriere V, Roussel L, Ortega N, *et al.* IL-33, the IL-1-like cytokine ligand for ST2 receptor, is a chromatin-associated nuclear factor *in vivo*. Proc Natl Acad Sci USA 2007;104:282–287.
26. Wang W, Tanaka T, Okamura H, *et al.* Interleukin-18 enhances the production of interleukin-8 by eosinophils. Eur J Immunol 2001;31:1010–1016.
27. Kumano K, Nakao A, Nakajima H, *et al.* Interleukin-18 enhances antigen-induced eosinophil recruitment into the mouse airways. Am J Respir Crit Care Med 1999;160:873–878.
28. Baskar P, Pincus SH. Selective regulation of eosinophil degranulation by interleukin 1β. Proc Soc Exp Biol Med 1992;199:249–254.
29. Kumar S, Tzimas MN, Griswold DE, *et al.* Expression of ST2, an interleukin-1 receptor homologue, is induced by proinflammatory stimuli. Biochem Biophys Res Commun 1997;235:474–478.
30. Meisel C, Bonhagen K, Lohning M, *et al.* Regulation and function of T1/ST2 expression on CD4+ T cells: induction of type 2 cytokine production by T1/ST2 cross-linking. J Immunol 2001;166:3143–3150.
31. Walsh GM, Hartnell A, Wardlaw AJ, *et al.* IL-5 enhances the *in vitro* adhesion of human eosinophils, but not neutrophils, in a leucocyte integrin (CD11/18)-dependent manner. Immunology 1990;71:258–265.

doi: 10.1111/j.1365-2222.2007.02761.x

ORIGINAL PAPER

Clinical and Experimental Allergy, **37**, 1334–1339

Mannose binding lectin gene polymorphisms and asthma

X. Wang*, J. Saito*, Y. Tanino*, T. Ishida*, T. Fujita† and M. Munakata*

*Departments of *Pulmonary Medicine and †Immunology, School of Medicine, Fukushima Medical University, Fukushima City, Japan*

Clinical and Experimental Allergy

Correspondence:
Mitsuru Munakata, Department of Pulmonary Medicine, School of Medicine, Fukushima Medical University, Hikarigaoka-1, Fukushima City 960-1295, Japan.
E-mail: munakata@fmu.ac.jp

Summary

Background Bronchial asthma is a chronic inflammatory disorder of the airways. Recently, it has been suggested that complement plays significant roles in asthma. Mannose-binding lectin (MBL) is one of the key molecules in complement activation pathways that are associated with several infectious and immune disorders.

Subjects and method To investigate whether MBL plays roles in asthma, we analysed *MBL2* polymorphisms (allele B, H/L and Y/X) and plasma MBL levels in a Japanese adult population including 232 healthy controls and 579 asthmatics.

Results Although there was linkage disequilibrium among the three polymorphisms, each polymorphism significantly affects serum MBL levels independently. However, there were no significant differences between asthmatics and controls in *MBL2* genotype distribution and in MBL concentrations [1.47 ± 0.07(SE) mg/L for asthmatics and 1.66 ± 0.14 mg/L for controls, $P = 0.2$]. MBL levels and genotype have no significant relationship with serum IgE, pulmonary functions, and the severity of asthma.

Conclusion Although plasma MBL levels depend on the *MBL2* polymorphisms, these polymorphisms and plasma MBL levels are not associated with the asthma phenotype.

Keywords adult, asthma, innate immunity, MBL, polymorphism
Submitted 20 September 2006; revised 24 April 2007; accepted 1 May 2007

Introduction

Bronchial asthma is a chronic inflammatory disorder of the airways characterized by the presence of reversible airflow obstruction, airway hyperresponsiveness (AHR), and airway remodelling [1]. Recently, there has been a great deal of research dealing with the role of innate immune mediators of the complement cascade, particularly the anaphylatoxins (C3a, C5a). C3a production at the airway surface has been suggested to serve as a common pathway for the induction of AHR to a variety of asthma triggers, such as allergens and viral infections. C5/C5a has dual immuno-regulatory roles: protecting against T-helper type 2-mediated immune responses during initiation of responses, and a pro-inflammatory role once immune responses are established [2]. On the other hand, respiratory infection caused by viruses, Chlamydia, and Mycoplasma has been implicated in the pathogenesis of asthma [3–5]. During infancy, certain viruses such as respiratory syncytial virus (RSV) have been speculated to have the potential to increase susceptibility to asthma [5]. It has also been proposed that certain bacterial infections, such as *Chlamydia pneumoniae* and *Mycoplasma pneumoniae*, may cause chronic airway inflammation [6]. These may be directly related to the aetiology of asthma or its chronicity, severity, and instability.

Mannose-binding lectin (MBL) is one of the C-type lectins, and is an important component of innate immunity. MBL binds to MBL-associated serine protease (MASP) 1 and 2 to initiate the complement cascade and to also enhance phagocytotic activity by opsonizing pathogens [7, 8]. MBL deficiency is associated with the susceptibility to and the severity of several infections and immune disorders [9–14]. The basal serum levels of normal MBL protein and biological activities are associated with single nucleotide polymorphisms (SNPs) in exon1 and promoter haplotypes [12, 15–18]. Three polymorphic sites, codon54 (GGC to GAC, allele B), codon57 (GGA to GAA, allele C), and codon52 (CGT to TGT, allele D), are situated in exon1 of *MBL2*. Population studies have shown that there are significant ethnic differences in the polymorphisms; several studies have reported that the codon54 SNP is common but that the other two SNPs are absent or extremely rare in the Japanese population [19]. Two other SNPs lie at promoters −550 (G/C, allele H/L) and −221 (G/C, allele Y/X) of *MBL2* and have been demonstrated to affect serum MBL levels in some studies [18].

Given this information, we wished to elucidate the role of MBL in the pathophysiology of asthma, and to examine the relationship among *MBL2* polymorphisms, plasma MBL levels, and asthma phenotype in a Japanese population.

Materials and methods

Subjects

A total of 811 adult subjects, including 579 asthmatics and 232 healthy controls, were involved in the study. All patients were recruited from six outpatient clinics including Fukushima Medical University Hospital (see Acknowledgement). Asthma was diagnosed based on the presence of at least one or more of the respiratory symptoms (recurrent cough, wheezing, or dyspnoea), increased airway responsiveness to methacholine or the presence of reversible airflow limitation, and the absence of other pulmonary diseases. The asthmatics were divided into those having atopic ($n = 437$) and those having non-atopic asthma ($n = 142$). Subjects who had serum non-specific IgE levels that were higher than 250 IU/mL or had at least one positive antigen-specific IgE determined by a RAST were considered to have atopy. Control subjects were normal, asymptomatic volunteers with no past history of asthma or other airway diseases. The age of the control subjects was not matched for asthmatics. Plasma was available for 355 asthmatics (257 atopic and 98 non-atopic asthmatics) and 100 controls. The clinical characteristics of the subjects are shown in Table 1. This study's protocol was approved by the ethical committees of Fukushima Medical University, and written informed consent was obtained from all the participants.

Genotyping

Blood samples were collected in tubes containing EDTA-Na_2 and were then frozen at $-80\,^{\circ}C$ before DNA preparation. Genomic DNA was extracted using DNA extraction kits according to the manufacturer's instructions (QIAamp DNA Blood Maxi Kit, Qiagen K. K., Tokyo, Japan). Genotyping of codon54 (GGC → GAC, allele A or B) was performed using a PCR–restriction fragment length polymorphism (RFLP) technique. Because allele C and allele D are absent or extremely rare in the Japanese population [19], only allele A or B was studied. For genotyping of promoter −550 (G → C, allele H or L) and −221(G → C, allele Y or X), the fluorogenic allele-specific TaqMan probes and primers (TaqMan SNP Genotyping Assays, Applied Biosystems, Foster, CA, USA) were used. Allelic discrimination was performed using the ABI Prism 7000 Sequence Detection System (Applied Biosystems).

Assay for mannose-binding lectin

The plasma samples collected from 355 patients and 100 controls were frozen to $-80\,^{\circ}C$ before measurements were taken. The plasma MBL concentration was measured using a commercially available ELISA kit (HyCult Biotechnology, Uden, the Netherlands).

Statistics

The χ^2 test was used to compare the genotype frequencies of asthmatic patients and controls. The promoter haplotype and combination between codon54 were analysed in case–control haplotype and linkage disequilibrium by SNP Analyze software (DYNACOM, Kanagawa, Japan). The Kruskall–Wallis test was used to examine the MBL level. Student's *t*-test was used to compare the mean age and non-specific IgE levels between asthmatic patients and controls. Values were presented as mean ± SE. Statistical evaluations were conducted using SPSS Base 11.0J and SPSS Regression Models 9.0J Windows (SPSS Inc., Tokyo, Japan). A *P*-value < 0.05 was considered to be statistically significant.

Results

Characteristics of the subjects (Table 1)

The characteristics of the subjects including the 579 asthmatic patients and the 232 controls are shown in

Table 1. Characteristics of the patients with asthma and controls in Japanese

	Age (mean ± SE)	Gender (M/F) (M%)	Age of onset (years old)	Log (IgE) (IU/L)	$FEV_{1.0}$ (L)	FEV_1%	V_{50} (L/s)	V_{25} (L/s)	*N*
Control	25.5 ± 0.6	104/128 (44.8)	–	1.85 ± 0.04	NA	NA	NA	NA	232
Asthma	49.6 ± 0.7*	293/286 (50.6)	32.2 ± 0.6	2.44 ± 0.03*	2.34 ± 0.04	73.5 ± 0.7	2.4 ± 0.1	0.90 ± 0.03	579
Atopic	46.0 ± 0.6	231/206 (52.9)**	27.7 ± 0.7	2.66 ± 0.03	2.45 ± 0.04	74.2 ± 0.7	2.6 ± 0.1	0.96 ± 0.03	437
Non-atopic	60.5 ± 0.8#	62/80 (43.7)	46.3 ± 1.0##	1.78 ± 0.05##	2.00 ± 0.06##	71.3 ± 1.5	2.0 ± 0.1##	0.68 ± 0.05##	142

*$P < 0.01$ vs. control.

**$P < 0.05$ vs. non-atopic asthma and control.

#$P < 0.01$ vs. atopic asthma and control.

##$P < 0.01$ vs. atopic asthma.

NA, not available; FEV, forced expiratory volume in one second.

Table 2. Distribution of mannose-binding lectin (MBL2) genotypes in asthmatics and controls

SNP	Genotype or allele	Asthma patients			Control	P-value*
		Atopic ($n = 437$)	Non-atopic ($n = 142$)	Total ($n = 579$)	($n = 232$)	
Codon54 (allele B)	Genotype					
	A/A	290 (66.4%)	99 (69.7%)	389 (67.2%)	157 (67.7%)	0.277
	A/B	126 (28.8%)	38 (26.8%)	164 (28.3%)	70 (30.2%)	
	B/B	21 (4.8%)	5 (3.5%)	26 (4.5%)	5 (2.2%)	
	Allele					
	B	168 (19.2%)	48 (16.9%)	216 (18.7%)	80 (17.2%)	0.506
Promoter						
−221 (allele X)	Genotype					
	Y/Y	341 (78.0%)	118 (83.1%)	459 (79.3%)	170 (73.3%)	0.165
	Y/X	90 (20.6%)	24 (16.9%)	114 (19.7%)	58 (25.0%)	
	X/X	6 (1.4%)	0	6 (1.0%)	4 (1.7%)	
	Allele					
	X	102 (11.7%)	24 (8.5%)	126 (10.1%)	66 (14.2%)	0.06
−550 (allele L)	Genotype					
	H/H	107 (24.5%)	33 (23.2%)	140 (24.2%)	44 (19.0%)	0.276
	H/L	217 (49.7%)	76 (53.5%)	293 (50.6%)	126 (54.3%)	
	L/L	113 (25.9%)	33 (23.2%)	146 (25.2%)	66 (26.7%)	
	Allele					
	L	443 (50.7%)	142 (50%)	585 (50.5%)	250 (53.9%)	0.221

*Compared with genotypes or allele frequency in asthmatics and controls.

Table 1. The mean age of the patients with asthma was 49.6 years (range 18–87 years old) and was significantly higher than the mean age of the control subjects (25.5 years) ($P < 0.01$). The patients with asthma had significantly higher non-specific IgE levels than controls ($P < 0.01$). The non-atopic asthmatics were older than atopic asthmatics, and had a later onset, a higher proportion of females ($P < 0.05$), and decreased pulmonary functions ($P < 0.01$).

Mannose-binding lectin 2 genotypes distribution (Table 2)

The data on these SNPs are shown in table 2. All the genotype distributions were fit to Hardy–Weinberg equilibrium. There was no significant difference in the genotype frequencies and each SNP between asthmatics and controls. The frequency of allele B were 18.7% in asthmatics and 17.2% in controls ($P = 0.51$), the frequencies of allele X were 10.1% and 14.2% ($P = 0.06$), and the frequencies of allele L were 50.5% and 53.9% in asthmatics and controls ($P = 0.22$), respectively. There was no significant difference in each allele frequency between asthmatics and controls. No significant difference was observed in the genotype and allele frequencies between the atopic and non-atopic asthmatics. We also compared the genotype distributions and allele frequencies according to gender, onset age of asthma, blood eosinophil cell count, serum IgE level and lung function [forced expiratory volume in one second (FEV_1) and FEV_1%]; however, no differences were observed (data not shown).

Mannose-binding lectin 2 haplotype and plasma mannose-binding lectin levels (Table 3)

Linkage disequilibria among two promoter variant loci and codon54 polymorphism were found in Japanese population. The promoter HH/YY and HL/YY haplotype combined with codon54 A/A are common in both asthmatics and controls (24.0% and 22.6% vs. 19.0% and 23.3%, respectively). These haplotypes were associated with a higher MBL concentration. In codon54 A/A genotype, LL/XY and LL/XX haplotypes were rare in both asthmatics and controls, and have lower MBL plasma levels. The codon54 A/B or B/B genotype with any combination of promoter haplotype was associated with lower MBL levels. Subjects with the BB/LL/YY haplotype have the lowest MBL concentration, and the BHX haplotype was absent in this study population. There was no difference in MBL2 haplotype distribution between asthmatics and controls. Also there was no difference in haplotype frequency between atopic and non-atopic asthmatics.

Plasma mannose-binding lectin levels and combinations between codon54 and promoter genotype (Fig. 1)

The plasma MBL concentration is shown in Fig. 1. Each individual with codon54 B/B or A/B genotype has significantly low MBL levels (0.03 ± 0.03 mg/L for the B/B and 0.29 ± 0.02 mg/L for the A/B vs. 2.17 ± 0.07 mg/L for the A/A, $P < 0.0001$). In subjects with codon54 A/A

Table 3. Distribution of mannose-binding lectin (MBL2) gene haplotype in asthmatics and controls

Codon54 genotype	Promoter haplotype	Asthma			Controls ($n = 232$)	MBL (mg/L) (mean ± SE)
		Atopic ($n = 437$)	Non-atopic ($n = 142$)	Total ($n = 579$)		
A/A	HH/YY	106 (24.3%)	33 (23.2%)	139 (24.0%)	44 (19.0%)	2.33 ± 0.1
	HL/YY	90 (20.6%)	41 (28.9%)	131 (22.6%)	54 (23.3%)	2.39 ± 0.1
	LL/YY	19 (4.3%)	6 (4.2%)	25 (4.3%)	8 (3.4%)	2.10 ± 0.3
	HL/XY	44 (10.1%)	9 (6.3%)	53 (9.2%)	33 (14.2%)	1.78 ± 0.2
	LL/XY	25 (5.7%)	10 (7.0%)	35 (6.0%)	14 (6.0%)	1.57 ± 0.1[#]
	LL/XX	6 (1.4%)	0	6 (1.0%)	4 (1.7%)	0.46 ± 0.1[*]
A/B	HH/YY	1 (0.2%)	0	1 (0.2%)	0	–
	HL/YY	81 (18.5%)	26 (18.3%)	107 (18.5%)	38 (16.4%)	0.37 ± 0.0[†]
	LL/YY	23 (5.3%)	7 (4.9%)	30 (5.2%)	21 (9.1%)	0.24 ± 0.0[†]
	HL/XY	1 (0.2%)	0	1 (0.2%)	1 (0.4%)	–
	LL/XY	20 (4.6%)	5 (3.5%)	25 (4.3%)	10 (4.3%)	0.02 ± 0.0[†]
B/B	HL/YY	1 (0.2%)	0	1 (0.2%)	0	–
	LL/YY	20 (4.6%)	5 (3.5%)	25 (4.3%)	5 (2.2%)	0.003 ± 0.0[†]
MBL sufficient		284 (65.0%)[‡]	99 (69.7%)	383 (66.1%)	153 (65.9%)	2.20 ± 1.15
MBL insufficient		153 (35.0%)[§]	43 (30.3%)	196 (33.9%)	79 (34.1%)	0.26 ± 0.21[¶]

[*] $P < 0.05$ vs. AAHHYY and AAHLYY.
[#] $P < 0.05$ vs. AAHLYY.
[†] $P < 0.01$ vs. AAHHYY, AAHLYY, AALLYY, AAHLXY and AALLXY.
[¶] $P < 0.01$ vs. MBL sufficient.
[‡] Haplotype: AA/HH/YY, AA/HL/YY, AA/LL/YY, AA/HL/XY and AA/LL/XY.
[§] Haplotype: AA/LL/XX, AB/HH/YY, AB/HL/YY, AB/LL/YY, AB/HL/XY, AB/LL/XY and BB/HL/YY and BB/LL/YY.

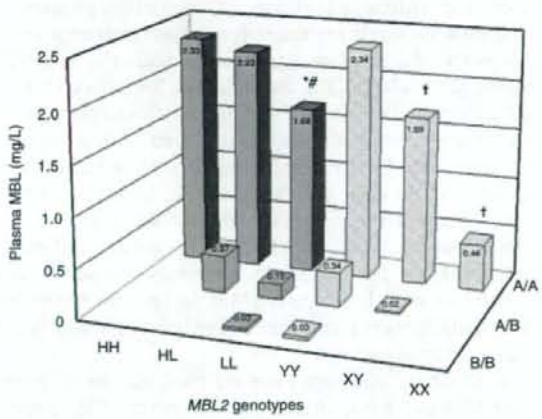

Fig. 1. Relation of plasma mannose-binding lectin (MBL) levels to *MBL2* gentypes and haplotypes. [*] $P < 0.01$ vs. AAHH haplotype; [#] $P < 0.05$ vs. AAHL haplotype; [†] $P < 0.01$ vs. AAYY haplotype.

genotype, the promoter −550 L/L genotype was associated with decreased MBL concentration (1.68 ± 0.14 mg/L) compared with the H/H (2.33 ± 0.12 mg/L, $P < 0.01$) or H/L (2.23 ± 0.09 mg/L, $P < 0.05$) genotype, and the promoter − 221 X/X or X/Y genotype was associated with a lower MBL concentration (0.46 ± 0.13 and 1.69 ± 0.11 mg/L, respectively) than the Y/Y genotype (2.34 ± 0.08 mg/L, $P < 0.01$). Accordingly, the plasma MBL concentration is determined independently with genotypes of all three SNPs. The mean plasma MBL levels of asthmatics (1.47 ± 0.07 mg/L) were not different from those of the controls (1.66 ± 0.14 mg/L), and atopic asthmatics (1.39 ± 0.08 mg/L) and non-atopic asthmatics (1.66 ± 0.13 mg/L) had similar plasma MBL levels. There was no significant relation between MBL concentration and gender, age, onset age of asthma, blood eosinophil cell count, serum IgE level, and lung function (FEV_1 and FEV_1%) (data not shown).

Discussion

In this study, we investigated MBL gene polymorphisms and plasma MBL levels in a relatively large adult Japanese population and examined the relationship between MBL and the asthma phenotype. There are linkage disequilibria within the codon54 and two promoter SNPs. All three *MBL2* polymorphisms affect plasma MBL levels independently and the codon54 genotypes have the strongest effect on plasma MBL levels in Japanese population. However, these polymorphisms and plasma MBL levels are not associated with asthma and related phenotypes.

The hypothesis that MBL may have significant roles in asthma has received much attention, because a significant amount of information suggests that innate immunity has a role in the susceptibility to and the pathophysiology of asthma [4, 5, 20]. MBL is a C-type serum lectin that specifically binds to carbohydrate structures on various microorganisms and mediates phagocytosis (opsonic efficacy) [7]. MBL binds to serine proteases called MASPs to

activate the complement lectin pathway [8]. It has been suggested that MBL has various roles in asthma mediated through two streams: complement activation itself and susceptibility to infectious agents.

In asthma, significant roles for anaphylatoxins (C3a, C5a), byproducts of complement activation, have been identified. C3a has long been known to activate mast cells, basophils, and eosinophils, as well as to cause smooth muscle contraction. C3a is generated in the lungs of asthmatic patients but not healthy subjects [21]. In murine models of allergic AHR and inflammation, airway responses are inhibited by complement activation and small molecule C3a receptor antagonists [22]. Furthermore, cell–cell interaction between airway smooth muscle and mast cells enhances C3a-induced mast cell degranulation, which likely regulates airway smooth muscle function; this suggests that C3a contributes to the pathogenesis of asthma [23, 24]. On the other hand, C5 is activated within the lungs after infection or exposure to allergen, and C5 inhibition has a profound effect on airway inflammation, AHR, and airway responses to antigen. C5a serves as a direct link between the innate immune system and the development of AHR by directly engaging its receptors that are expressed in the airways [20]. In addition, respiratory infections caused by viruses, Chlamydia, and Mycoplasma have been suggested to be linked with the pathogenesis of asthma [5]. During infancy, certain viruses, such as RSV, are implicated as being potentially responsible for the inception of the asthmatic phenotype [5, 25]. MBL might be involved in patients' susceptibility to such infections.

Several studies have investigated the association between MBL and asthma, although most of these were carried out in childhood asthma. In children, MBL deficiency enhanced the risk of infections and was involved in acute exacerbations of asthma [26–28]. Nagy et al. [26] concluded that the variant *MBL2* alleles play an important role in the susceptibility of children to asthma, especially in association with *C. pneumoniae* infection. These studies suggest that a defect or reduction of MBL facilitates asthma. Uguz A. et al. compared the serum MBL levels in 72 asthmatic children and 30 controls; they found significantly increased serum MBL levels in the asthmatic children and a significant correlation between MBL and blood eosinophils [28], suggesting that increased oxidative stress in asthmatic airways stimulates MBL synthesis and results in complement activation. This activation may contribute to the airway inflammation seen in asthma. Kaur et al. [29] and Leung et al. [30] have reported a similar association . In the mouse asthma model induced by *Aspergillus fumigatus*, similar results were reported. Hogaboam et al. [31] examined the effect of MBL-A deficiency and found that MBL-A contributed to the development and maintenance of AHR, but not to the development of airway remodelling. The results of the above studies are somewhat contradictory. However, in the clinical studies, the number of subjects examined was small, which makes it difficult to arrive at definite conclusions. In adult asthma, there is only one study reported by Aittoniemi et al. [32] that involved 137 atopic and 104 non-atopic asthmatics dealing with these issues. They examined *MBL2* polymorphism in adult asthmatics and found that the presence of variant allele X and low MBL expression were risk factors for asthma only in non-atopic males; however, MBL had no effect on the occurrence of atopy. There was no significant difference in the frequency of allele X between non-atopic males and non-atopic controls (8.1% and 11.9%, respectively, $P = 0.285$) in our study.

In the present study, we examined 579 adult asthmatic subjects (437 atopic and 142 non-atopic asthmatics) in whom detailed clinical information, including pulmonary functions, serum IgE, peripheral eosinophil count, and treatment history, was available. The results of our study indicate that *MBL2* polymorphisms and haplotypes are not associated with susceptibility to asthma, serum IgE levels, or peripheral eosinophil counts. In addition, plasma MBL levels have no clear relationship with age, age of onset, duration, and the severity of asthma. Therefore, the MBL genotypes and plasma MBL levels are not associated with the asthma phenotype in the adult population. Plasma MBL levels are dependent on age; children under 15 years of age have significantly higher serum MBL levels than adults [33]. In addition, the effect of MBL deficiency on the susceptibility to infectious agents seems to be age-dependent, because children with MBL deficiency tend to be more susceptible to such infections than adults with the same deficiency. In this study, plasma MBL levels showed no significant change according to age, suggesting that plasma MBL levels remain unchanged when subjects become adults. Given these findings, it is possible that the link between MBL and asthma phenotype gradually weakens as subjects become older and is not observed in adulthood.

In summary, although there are good reasons to suspect that MBL has a role in asthma, the results of the present study suggest that the asthma phenotype is independent of the MBL2 genotypes and plasma MBL levels, at least in the adult population.

Acknowledgements

The authors express their sincere gratitude to the following doctors who agreed to share the blood and DNA samples of asthmatic patients for this study: Akira Ishii, MD, School of Medicine Tokyo University, Ken Ohta, MD, School of Medicine Teikyo University, Nobuyuki Hizawa, MD, School of Medicine of Hokkaido University, Nobuyuki Kobayashi, MD, International Medical Center of Japan, Yasuyuki Sano, MD, The Fraternity Memorial Hospital,

Shunnsuke Shoji, MD, Fukuoka National Hospital, and Yoshio Uehara, MD, Health Service Center of Tokyo University.

References

1 *Annonimus: Global Initiative for Asthma, Global Strategy for Asthma Management and Prevention. NIH Publication, No. 02-3659.* USA: NHLBI/WHO, 2003.

2 Wills-Karp M, Koehl J. New insights into the role of the complement pathway in allergy and asthma. *Curr Allergy Asthma Rep* 2005; 5:362–9.

3 Hahn DL, Dodge RW, Golubjatnikov R. Association of *Chlamydia pneumoniae* (strain TWAR) infection with wheezing, asthmatic bronchitis, and adult-onset asthma. *JAMA* 1991; 266:225–30.

4 Johnston SL, Pattemore PK, Sanderson G *et al.* The relationship between upper respiratory infections and hospital admissions for asthma: a time-trend analysis. *Am J Respir Crit Care Med* 1996; 154 (Part 1):654–60.

5 Lemanske RF Jr. Is asthma an infectious disease? Thomas A. Neff lecture. *Chest* 2003; 123 (Suppl.):385S–90S.

6 Kraft M, Cassell GH, Henson JE *et al.* Detection of *Mycoplasma pneumoniae* in the airways of adults with chronic asthma. *Am J Respir Crit Care Med* 1998; 158:998–1001.

7 Matsushita M, Fujita T. Activation of the classical complement pathway by mannose-binding protein in association with a novel C1s-like serine protease. *J Exp Med* 1992; 176:1497–502.

8 Fujita T, Matsushita M, Endo Y. The lectin-complement pathway – its role in innate immunity and evolution. *Immunol Rev* 2004; 198:185–202.

9 Kilpatrick DC. Mannan-binding lectin: clinical significance and applications. *Biochim Biophys Acta* 2002; 1572:401–13.

10 Turner MW, Hamvas RM. Mannose-binding lectin: structure, function, genetics and disease associations. *Rev Immunogenet* 2000; 2:305–22.

11 Super M, Thiel S, Lu J, Levinsky RJ, Turner MW. Association of low levels of mannan-binding protein with a common defect of opsonisation. *Lancet* 1989; 2:1236–9.

12 Sumiya M, Super M, Tabona P *et al.* Molecular basis of opsonic defect in immunodeficient children. *Lancet* 1991; 337:1569–70.

13 Koch A, Melbye M, Sorensen P *et al.* Acute respiratory tract infections and mannose-binding lectin insufficiency during early childhood. *JAMA* 2001; 285:1316–21.

14 Cedzynski M, Szemraj J, Swierzko AS *et al.* Mannan-binding lectin insufficiency in children with recurrent infections of the respiratory system. *Clin Exp Immunol* 2004; 136:304–11.

15 Lipscombe RJ, Sumiya M, Hill AV *et al.* High frequencies in African and non-African populations of independent mutations in the mannose binding protein gene. *Hum Mol Genet* 1992; 1:709–15.

16 Turner MW, Lipscombe RJ, Levinsky RJ *et al.* Mutations in the human mannose binding protein gene: their frequencies in three distinct populations and relationship to serum levels of the protein. *Immunodeficiency* 1993; 4:285–7.

17 Madsen HO, Garred P, Kurtzhals JA *et al.* A new frequent allele is the missing link in the structural polymorphism of the human mannan-binding protein. *Immunogenetics* 1994; 40:37–44.

18 Madsen HO, Garred P, Thiel S *et al.* Interplay between promoter and structural gene variants control basal serum level of mannan-binding protein. *J Immunol* 1995; 155:3013–20.

19 Tsutsumi A, Sasaki K, Wakamiya N *et al.* Mannose-binding lectin gene: polymorphisms in Japanese patients with systemic lupus erythematosus, rheumatoid arthritis and Sjogren's syndrome. *Genes Immunol* 2001; 2:99–104.

20 Peng T, Hao L, Madri JA *et al.* Role of C5 in the development of airway inflammation, airway hyperresponsiveness, and ongoing airway response. *J Clin Invest* 2005; 115:1590–600.

21 Ali H, Panettieri RA Jr. Anaphylatoxin C3a receptors in asthma. *Respir Res* 2005; 6:19.

22 Taube C, Rha YH, Takeda K *et al.* Inhibition of complement activation decreases airway inflammation and hyperresponsiveness. *Am J Respir Crit Care Med* 2003; 168:1333–41.

23 Brightling CE, Bradding P, Symon FA, Holgate ST, Wardlaw AJ, Pavord ID. Mast-cell infiltration of airway smooth muscle in asthma. *N Engl J Med* 2002; 346:1699–705.

24 Thangam EB, Venkatesha RT, Zaidi AK *et al.* Airway smooth muscle cells enhance C3a-induced mast cell degranulation following cell-cell contact. *FASEB J* 2005; 19:798–800.

25 Landau LI. Bronchiolitis and asthma: are they related? *Thorax* 1994; 49:293–6.

26 Nagy A, Kozma GT, Keszei M, Treszl A, Falus A, Szalai C. The development of asthma in children infected with *Chlamydia Pneumoniae* is dependent on the modifying effect of mannose-binding lectin. *J Allergy Clin Immunol* 2003; 112:729–34.

27 Thorarinsdottir HK, Ludviksson BR, Vikingsdottir T *et al.* Childhood levels of immunoglobulins and mannan-binding lectin in relation to infections and allergy. *Scand J Immunol* 2005; 61:466–74.

28 Uguz A, Berber Z, Coskun M, Halide Akbas S, Yegin O. Mannose-binding lectin levels in children with asthma. *Pediatr Allergy Immunol* 2005; 16:231–5.

29 Kaur S, Gupta VK, Shah A, Thiel S, Sarma PU, Madan T. Elevated levels of mannan-binding leptin (MBL) and eosinophilia in patients of bronchial asthma with allergic rhinitis and allergic bronchopulmonary aspergillosis associate with a novel intronic polymorphism in MBL. *Clin Exp Immunol* 2006; 143:414–9.

30 Leung TF, Tang NL, Sung YM *et al.* Genetic association study between mbl2 and asthma phenotypes in Chinese children. *Pediatr Allergy Immunol* 2006; 17:501–7.

31 Hogaboam CM, Takahashi K, Ezekowitz RA, Kunkel SL, Schuh JM. Mannose-binding lectin deficiency alters the development of fungal asthma: effects on airway response, inflammation, and cytokine profile. *J Leukoc Biol* 2004; 75:805–14.

32 Aittoniemi J, Soranummi H, Rovio AT *et al.* Mannose-binding lectin 2 (MBL2) gene polymorphism in asthma and atopy among adults. *Clin Exp Immunol* 2005; 142:120–4.

33 Aittoniemi J, Miettinen A, Laippala P *et al.* Age-dependent variation in the serum concentration of mannan-binding protein. *Acta Paediatr* 1996; 85:906–9.

Positioning of autoimmune TCR-Ob.2F3 and TCR-Ob.3D1 on the MBP85–99/HLA-DR2 complex

Zenichiro Kato[†‡§¶‖], Joel N. H. Stern[†], Hironori K. Nakamura[§], Kazuo Kuwata[§], Naomi Kondo[‡§¶], and Jack L. Strominger[†‖]

[†]Department of Molecular and Cellular Biology, Harvard University, Cambridge, MA 02138; and [‡]Department of Pediatrics, Graduate School of Medicine, [§]Center for Emerging Infectious Diseases, and [¶]Center for Advanced Drug Research, Gifu University, 1-1 Yanagido, Gifu 5010-1194, Japan

Contributed by Jack L. Strominger, August 11, 2008 (sent for review July 8, 2008)

Since the first determination of structure of the HLA-A2 complex, >200 MHC/peptide structures have been recorded, whereas the available T cell receptor (TCR)/peptide/MHC complex structures now are <20. Among these structures, only six are TCR/peptide/MHC Class II (MHCII) structures. The most recent of these structures, obtained by using TCR-Ob.1A12 from a multiple sclerosis patient and the MBP85–99/HLA-DR2 complex, was very unusual in that the TCR was located near the N-terminal end of the peptide-binding cleft of the MHCII protein and had an orthogonal angle on the peptide/MHC complex. The unusual structure suggested the possibility of a disturbance of its signaling capability that could be related to autoimmunity. Here, homology modeling and a new simulation method developed for TCR/peptide/MHC docking have been used to examine the positioning of the complex of two additional TCRs obtained from the same patient (TCR-Ob.2F3 or TCR-Ob.3D1 with MBP85–99/HLA-DR2). The structures obtained by this simulation are compatible with available data on peptide specificity of the TCR epitope. All three TCRs from patient Ob including that from the previously determined crystal structure show a counterclockwise rotation. Two of them are located near the N terminus of the peptide-binding cleft, whereas the third is near the center. These data are compatible with the hypothesis that the rotation of the TCRs may alter the downstream signaling.

human leukocyte antigen | multiple sclerosis | myelin basic protein | structural docking | signaling

The elucidation of structures of protein complexes is an arduous procedure particularly when the complexes are very large. The production of protein by recombinant techniques and subsequent crystallization of the complexes followed by x-ray diffraction analysis is a standard method. Structures can also be determined by NMR but that technique is presently limited to only relatively small proteins or complexes not >40–50 kDa. The third method, simulation of structures by homology modeling, has improved greatly in recent years. However, this technique is usable only when an appropriate template structure is available.

Crystallization and structure determination by x-ray diffraction of a MHC-encoded Class I (MHCI) protein/peptide complex was first accomplished in 1987 and MHCII in 1993 (1, 2). Since then, >200 structures of such complexes have been recorded (3). The β chain of the TCRs that recognize these complexes were first cloned in 1984 (4, 5), and the first structure of a TCR chain was published in 1995 (6). Approximately 40 complete TCR structures including both α and β chains are available now (3, 7). Similarly, the first TCR/peptide/MHC complex structures were published in 1996 (8, 9) but the number of such complex structures available now is <20 (3). Among these, only six are TCR/peptide/MHCII structures. The most recent of these structures is very unusual in that the TCR was located near the N-terminal end of the peptide-binding cleft of the MHCII protein and its orthogonal angle on the MHCII/peptide was 84° as compared with a diagonal angle of 40–53° for the other five structures (10). Also, it was rotated counterclockwise on the MHC molecule relative to the other structures. This unusual structure suggested the possibility of a disturbance of its signaling capability that could be related to autoimmunity because this TCR, termed Ob.1A12 had been obtained from an autoreactive clone derived from a patient with multiple sclerosis (10). In fact, eight clones were obtained from this patient, two of which represent unique isolates (TCR-Ob.1A12 and TCR-Ob.3D1) and six of which have identical sequences, TCR-Ob.2F3 being an example (11).

In this article, we have used homology modeling of TCR structures on the appropriate templates and a new simulation method developed for TCR/peptide/MHC docking to examine the structures of the TCR/peptide/MHCII complexes of TCR-Ob.2F3 and TCR-Ob.3D1 in complex with the same MHC/peptide, namely HLA-DR2 (DRB1*1501/DRA) binding the myelin basic protein peptide epitope MBP85–99. MBP85–99 has previously been identified as the autoreactive peptide epitope in humans (12).

Results and Discussion

The AutoDock procedure was originally developed for docking studies of small chemicals to their receptors, for example the docking of a substrate to an enzyme (13). It makes use of charge and hydrophobicity calculations for both the receptor and the ligand (see *Materials and Methods*). By using this method in the present context, the peptide in question was first docked to the appropriate MHC molecule and separately to the TCR protein. The conformation of the peptide used in the docking in each case was taken from the crystal structure of the MBP85–99/HLA-DR2 (DRB1*1501, DRA) complex (10). After TCR/peptide and peptide/MHC structures were simulated, the two structures were merged by using the conformation of the peptide as the basis for merging. To validate the procedure, the technique was carried out by using two known TCR/peptide/MHC structures, that of the HLA-DR1 (DRB1*0101/DRA)/hemagglutinin (HA) 306–318 molecule in complex with the HLA-DR1-restricted HA306–318-specific TCR-HA1.7 (PDB ID code 1FYT) and then of the HLA-DR2/MBP85–99 molecule in complex with TCR-Ob.1A12 (PDB ID code 1YMM).

Simulated Structure of the TCR-HA1.7/HA306–318/HLA-DR1 Complex and the TCR-Ob.1A12/MBP85–99/HLA-DR2 Complex. The docking of HA306–318 to HLA-DR1 was simulated 10 times. Six of the 10 simulations showed exactly the same conformation inside the peptide-binding groove with energy equal to −33.8 kcal/mol (Fig. 1*A*). Four of the 10 showed different conformations binding outside of the groove with higher energies of −5.59, −5.59,

Author contributions: Z.K., J.N.H.S., K.K., N.K., and J.L.S. designed research; Z.K. and H.K.N. performed research; Z.K. and H.K.N. analyzed data; and Z.K., J.N.H.S., and J.L.S. wrote the paper.

The authors declare no conflict of interest.

‖To whom correspondence may be addressed. E-mail: zenkato@mac.com or jlstrom@fas.harvard.edu.

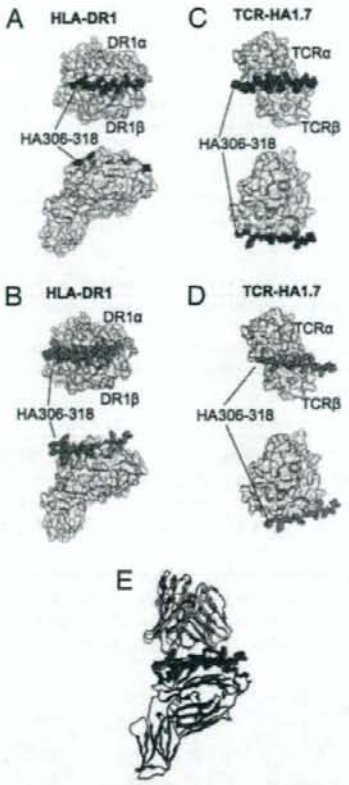

Fig. 1. Docking simulation of the HA306–318 peptide on HLA-DR1 and on TCR-HA1.7. (*A*) The six clustered docked peptides of HA306–318 on HLA-DR1 are indicated as space filling models in brown. (*B*) The four nonclustered docked peptides are indicated as space filling models in yellow. In *A* and *B*, HLA-DR1 (DRB1*0101/DRA) (20) is shown as a surface model in white. (*C*) The nine clustered docked peptides of HA306–318 on TCR-HA1.7 are indicated as space filling models in brown. (*D*) The one nonclustered docked peptide is shown as a space-filling model in yellow. In *C* and *D*, TCR-HA1.7 is shown as a surface model in white. (*E*) Merging of the docked TCR-HA1.7/HA306–318 and HA306–318/HLA-DR1 was carried out by using the conformation of the peptide as the basis for merging. Superposition was performed between the docked structure and the crystal structure of TCR-HA1.7/HA306–318/HLA-DR1 (20). Docked structure of TCR-HA1.7 in cyan, HA306–318 in brown, and crystal structures of both TCR-HA1.7 and HLA-DR1 in blue. The two TCR structures were superimposed by means of structures of HA306–318.

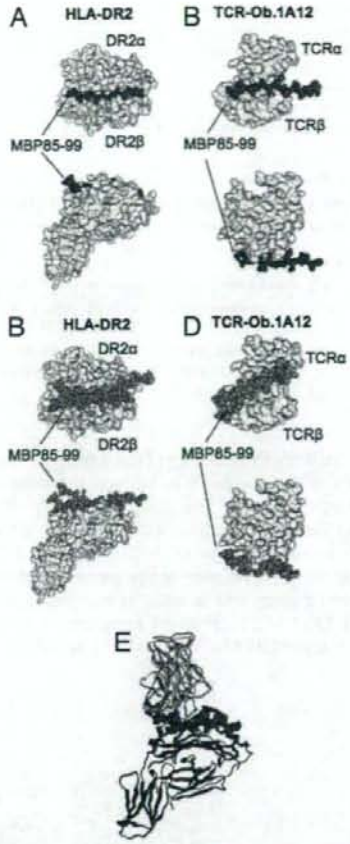

Fig. 2. Docking simulation of the MBP85–99 peptide on HLA-DR2 and on TCR-Ob.1A12. (*A*) The four clustered docked peptides of MBP85–99 on HLA-DR2 are indicated as space filling models in brown. (*B*) The six nonclustered docked peptides are indicated as space filling models in yellow. In *A* and *B*, HLA-DR2 (DRB1*1501/DRA) (10) is shown as a surface model in white. (*C*) The six clustered docked peptides of MBP85–99 on TCR-Ob.1A12 are indicated as space filling models in brown. (*D*) The four nonclustered docked peptides are indicated as space filling models in yellow. In *C* and *D*, TCR-Ob.1A12 is shown as a surface model in white. (*E*) Merging of the docked TCR-Ob.1A12/MBP85–99 and MBP85–99/HLA-DR2 was carried out by using the conformation of the peptide as the basis for merging. Superposition was performed between the docked structure and the crystal structure of TCR-Ob.1A12/MBP85–99/HLA-DR2 (10). Docked structure of TCR-Ob.1A12 in cyan, MBP85–99 in brown, and crystal structures of both TCR-Ob.1A12 and HLA-DR2 in blue. The two TCR structures were superimposed by means of structures of MBP85–99.

−5.68 and −8.73 kcal/mol (Fig. 1*B*). One of the clustered conformations inside the groove with the lowest energy was selected as representative.

Similarly, HA306–318 docking to TCR-HA1.7 was simulated 10 times. Nine of the 10 simulations had almost the same conformation with energy equal to −5.59 kcal/mol five times and energy −5.67 four times (Fig. 1*C*). One of the 10 simulations yielded a different conformation with a higher energy of −5.02 kcal/mol (Fig. 1*D*). Again, one of the five clustered conformations with the lowest energy was selected as representative.

Next, the TCR-HA1.7/HA306–318 simulated complex was merged with the HA306–318/HLA-DR1 simulated complex to give the TCR-HA1.7/HA306–318/HLA-DR1 complex by using the structure of the peptide as the basis for merging (a related procedure was used in a docking study of the dimeric maltose-binding complex involving maltose-binding protein and aspartate receptor, although in this case the octapeptide used was from a functional region of the maltose-binding protein) (14).

This simulated structure of the ternary complex was merged with the structure determined by crystallization and x-ray diffraction and gave excellent reproducibility with a rmsd of 1.64 Å (Fig. 1E). The same procedure was carried out to obtain the TCR-Ob.1A12/MBP85–99/HLA-DR2 structure. The docking of MBP85–99 to HLA-DR2 was simulated 10 times. Four of the 10 simulations showed exactly the same conformations inside the peptide-binding groove with energy equal to −26.8 kcal/mol (Fig. 2*A*). Six of the 10 showed binding outside of the groove each with a different conformation and with much higher energies of −3.02, −4.95, −4.95, −5.54, −5.64 and −5.91 kcal/mol (Fig. 2*B*). One of the clustered conformations inside the groove with the lowest energy was selected as representative.

Fig. 3. Sequence alignment of TCR-Ob.2F3 and TCR-Ob.3D1 with TCR-Ob.1A12. (*A*) Sequence alignment between TCR-Ob.2F3 and TCR-Ob.1A12. (*B*) Sequence alignment between TCR-Ob.3D1 and TCR-Ob.1A12. Differences in amino acids between the two clones are indicated in yellow. *, identical amino acids; +, similar amino acids.

Similarly, MBP85–99 docking to TCR-Ob.1A12 was simulated 10 times. Six of the 10 simulations had almost the same conformation with energy equal to −4.78 five times and energy −4.65 once (Fig. 2*C*). Four of the 10 simulations each yielded a different conformation with a similar energy of −4.50, −5.08, −5.32, and −5.32 kcal/mol (Fig. 2*D*). Again, one of the six clustered conformations with the lowest energy was selected as representative.

The TCR-Ob.1A12/MBP85–99 simulated complex was also merged with the MBP85–99/HLA-DR2 simulated complex as described above to give the TCR-Ob1A12/MBP85–99/HLA-DR2 complex. Merging of the simulated structure with the structure determined by x-ray crystallography gave excellent reproducibility with a rmsd of 1.54 Å (Fig. 2*E*). Thus, by using two known TCR/peptide/MHC complexes, these data provided a validation for the docking procedure used.

Notably, the energies of docking of the two peptides to their respective MHC proteins (−34 and −27 kcal/mol) were much lower than the energies of their docking to their respective TCR (−5.6

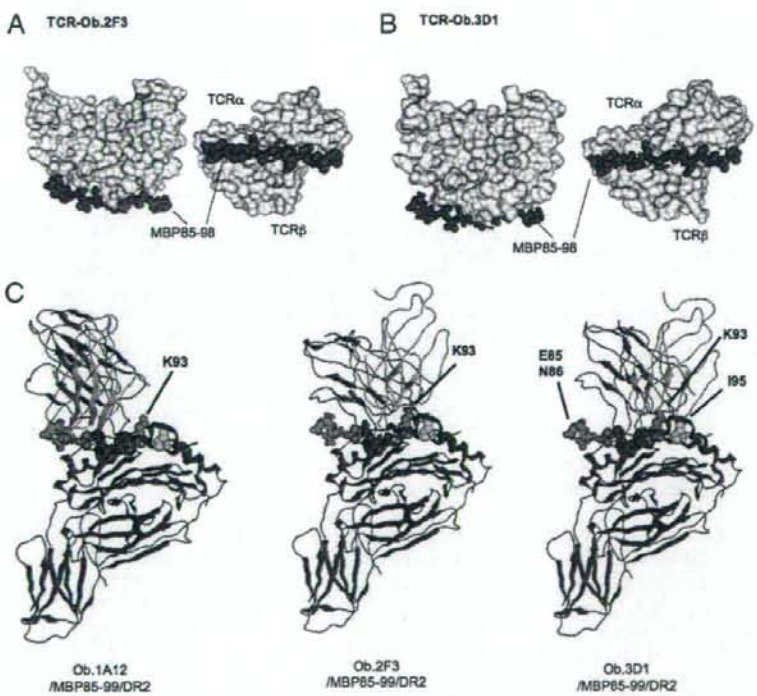

Fig. 4. Positioning of TCR-Ob.2F3 and TCR-Ob.3D1 on MBP85–99/HLA-DR2. (*A*) Docking simulation of the MBP85–99 peptide on TCR-Ob.2F3. The 10 clustered docked peptides are indicated as space filling models in brown. TCR-Ob.2F3 is shown as a surface model in white. (*B*) Docking simulation of the MBP85–99 peptide on TCR-Ob.3D1. The 10 clustered docked peptides are indicated as space filling models in brown. TCR-Ob.3D1 is shown as a surface model in white. (*C*) Comparison of positioning of the TCRs obtained from patient Ob. on the MBP85–99/HLA-DR2 structure. The structures of TCRs, MBP85–99 and HLA-DR2 (DRB1*1501/DRA) are shown as ribbon models. MBP85–99 and HLA-DR2 in blue, the α chains of the three TCRs in yellow, and the β chains of the three TCRs in red. Functionally important residues of MBP85–99 are shown as space filling models, E85 and N86 in green, V88 and K93 in orange, H90 and F91 in red, and I95 in yellow (see *Results and Discussion*).

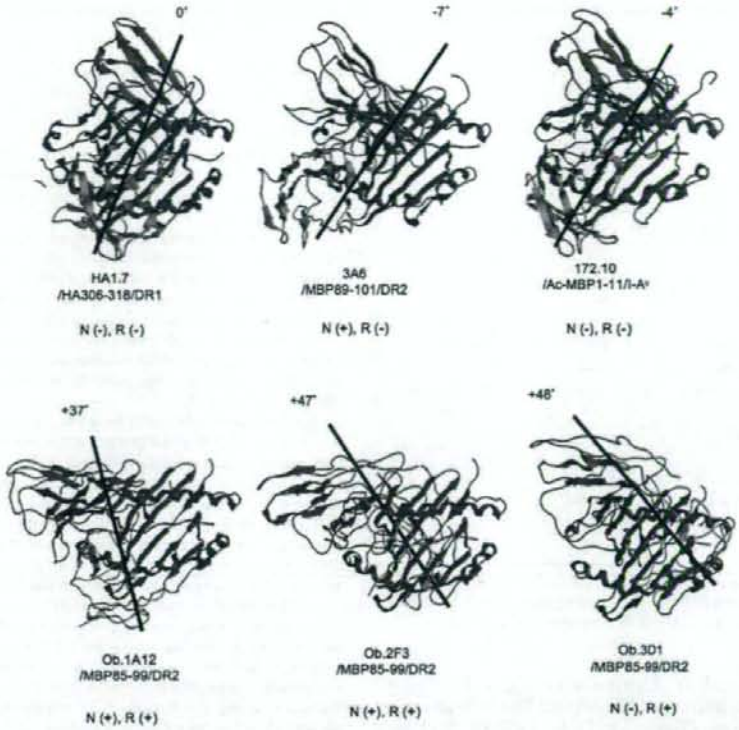

Fig. 5. Comparison of positioning between autoimmune TCRs and nonautoimmune TCR. HA1.7/HA306–318/DR1 indicates the positioning of a nonautoimmune TCR. All of the others are autoimmune TCRs. Black lines are drawn between the S–S bonds of TCRα and TCRβ. Coloring is the same as in Fig. 4*C*. N, N-terminal shift; R, counterclockwise rotation. The degrees of rotation taking TCR-HA1.7 on HA306–318/HLA-DR1 as 0° were as follows: TCR-3A6, −7°; TCR-172.10, −4°; TCR-Ob.1A12, +37°; Ob.2F3, +47°; and TCR-Ob.3D1, +48°.

and −4.8 kcal/mol). Thus, the binding of the peptide to the MHC proteins is much stronger than the binding to the TCR (13).

Simulated Structure of the TCR-Ob.2F3/MBP85–99/HLA-DR2 Complex and the TCR-Ob.3D1/MBP85–99/HLA-DR2 Complex. Next, structures of two TCR complexes from patient Ob whose complexes with HLA-DR2/MBP85–99 had not been determined were modeled. The sequence alignment with the template TCR-Ob.1A12 of these two TCRs, TCR-Ob.2F3 and TCR-Ob.3D1, are shown in Fig. 3. Notably, TCR-Ob.2F3 has 99% sequence identify with TCR-Ob.1A12 differing at only three amino acid positions. One of these is near the CDR3 loop of the TCR α chain and the other two are in the CDR3 loop of the TCR β chain. By contrast, TCR-Ob.3D1 had only 89% identify in the TCR α chain differing from TCR-Ob.1A12 by 10 positions including two gaps. It had only 37% identify (but 59% similarity) in the β chain differing from the template structure by 40 aa including two insertions in the CDR3 loop.

When MBP85–99 was docked to the modeled TCR-Ob.2F3, the 10 simulations showed almost the same conformation with energies of −5.77 kcal/mol five times, −5.76 four times, and −5.75 once (Fig. 4*A*). One of the clustered confirmations with the lowest energy was again selected as representative. The TCR-Ob.2F3/MBP85–99 docked structure was merged with the crystal structure of MBP85–99/HLA-DR2 again by using the conformation of the MBP85–99 peptide as the basis for merging.

Similarly, MBP85–99 was docked to the model TCR-Ob.3D1 10 times. All 10 simulations showed exactly the same conformation with energy −8.2 kcal/mol (Fig. 4*B*). One of these clustered conformations was again selected as representative and as before docked with the MBP85–99/HLA-DR2 structure.

The structural models that resulted form these simulations are shown in Fig. 4*C*. Several features are obvious. First, like TCR-Ob.1A12 (10), TCR-Ob.2F3 is positioned toward the N-terminus of the peptide-binding groove. However, it is located very slightly more toward the C-terminal end of the peptide. With regard to rotation, the counterclockwise rotation of Ob.1A12 (+37°) as compared with HA1.7 (taken as 0°) is apparent (Fig. 5). The TCR-Ob.2F3 had an even greater counterclockwise rotation (+47°).

TCR-Ob.3D1 by contrast was located near the middle of the peptide-binding cleft at the apex of the helixes in a similar position to TCR-HA1.7 (Figs. 4*C* and 5). However, again its counterclockwise rotation with regard to TCR-HA1.7 was large (+48°) and similar to that of TCR-Ob.2F3. When viewed from the top, the orthogonal angle of all three TCRs was distinct from that of HA1.7 and the other TCR/peptide/MHC complexes whose structures had been determined (5, 3, 15, 16). All three autoimmune TCRs show a counterclockwise rotation and two of them are located near the N-terminus of the peptide-binding cleft. These data are compatible with the hypothesis (10) that the rotation of the TCRs may alter the downstream signaling.

Available data on peptide specificity of the TCR epitope are compatible with these structures (Table 1, compiled from refs. 11, 12, 17, 18). With regard to the peptide, both TCR-Ob.1A12 and TCR-Ob.2F3 are sensitive to deletion of the N-terminal residue 85 of MBP85–99, whereas TCR-Ob.3D1 can recognize even a truncation of two residues at the N-terminus of

Table 1. Characters of the T cell clones from patient Ob

Clone	Ob.1A12	Ob.2F3	Ob.3D1
		Ob.1C3 Ob.1E10 Ob.1E12 Ob.1H8 Ob.2G9	
Minimal peptide	MBP 85–98	MBP 85–98	MBP 87–98
MBP 85–99	++++	++++	++++
MBP 85–98	++++	++++	++++
MBP 86–98	–	–	++++
MBP 87–98	–	–	++++
MBP 87–97	–	–	–
TCR epitope			
Major	HF—	HF-K–	HF-K–
Minor	—K–	—I	
MBP 85–99	++++	++++	++++
Val88Ala	++++	++++	ND
His90Ala	+	–	–
Phe91Ala	–	–	–
Lys93Ala	++++	++	–
Asn94Ala	++++	+++	+
Ile95Ala	++++	+++	++
Val96Ala	++++	++++	++++

Plus symbol indicates the proliferation of the T cell clones. ND, Not determined. These data are derived from Wucherpfennig *et al.* (11), Wucherpfennig *et al.* (12), Hausmann *et al.* (17), and Wucherpfennig *et al.* (18).

MBP85–99 (Figs. 4*C* and 5). Alanine scanning of MBP85–99 revealed that TCR recognition of His-90 and Phe-91 was essential for all three clones (Table 1). Only TCR-Ob.3D1 was sensitive to mutation of Asn-94 (P6) or partially Ile-95 (P7), however, K93 was not essential for TCR-Ob.1A12, and K93A revealed reduced sensitivity at this residue for TCR-Ob.2F3 (Table 1). However, both K93A and N94A eliminated reactivity with TCR-Ob.3D1 and I95A reduced reactivity. These data are compatible with the positions of the three TCR as shown in Figs. 4*C* and 5. Thus, good structure-function correlations are observed in the three autoimmune T cell clones.

The CD4 coreceptor binds to the membrane-proximal MHCII domains and is essential for T cell development and T cell function by recruiting the tyrosine kinase Lck. The alignment of the TCRs observed here showed that the geometry of the interaction with the CD4 coreceptor is altered for the TCRs as previously suggested (10). These findings raise the possibility that CD4 function is affected in immature T cells by an altered geometry of TCR binding to peptide-MHC during the formation of immunological synapses (10). These structures may add to our understanding of the molecular mechanism that could relate to autoimmunity.

Materials and Methods

Structure Modeling of TCR. Structural modeling of TCR-Ob.2F3 and TCR-Ob.3D1 was performed by using MOE software (Chemical Computing Group, www.chemcomp.com) combined with the segment-matching procedure (19, 20). Briefly, the structure of TCR-Ob.1A12 complexed with MBP85–99/HLA-DR2 (10) (PDB ID code 1YMM) was used as a template for homology modeling of TCR-Ob.2F3 and TCR-Ob.3D1. The modeled structure was further energy minimized (MOE software).

Docking Studies of the TCR with Peptide/MHC. Docking was performed by using the AutoDock software package running on Intel-based Xeon, ppcDarwin platform (13). The structure of HLA-DR1 (DRB1*0101/DRA), HLA-DR2 (DRB1*1501/DRA), TCR-HA1.7, TCR-Ob.1A12, TCR-Ob.2F3, or TCR-Ob.3D1 was used as the target structure. HA306–318 or MBP85–99 in the conformation found in their crystal structures (10, 21) was used as the ligand structure. AutoDock with a Lamarckian genetic search algorithm (LGA) was chosen for all dockings (13).

The optimized AutoDocking run parameters were similar to those described in ref. 13 with minor modification in grid size, a maximum number of energy evaluations, and a maximum number of generations. The proteins and ligands in the dockings were treated by using the united-atom approximation. Only polar hydrogens were added to the protein, and Kollman united-atom partial charges were assigned. All waters were removed. Atomic solvation parameters and fragmental volumes were assigned to the protein atoms by using an AUTODOCK utility, ADDSOL and the grid maps were calculated by using AUTOGRID (13).

The dimensions of the grids for docking were thus $180 \times 80 \times 90$ points (67.5 Å $\times$ 30.0 Å $\times$ 33.7 Å) and a grid-point spacing of 0.375 Å, and the center of the grids were placed to cover the surface of the HLA or TCR structure. The ligand was treated initially as all atom entities, i.e., all hydrogens were added, then partial atomic charges were calculated by using the Gasteiger-Marsilli method (13). AUTOTORS, an AUTODOCK utility, was used to define the rotable bonds in the ligand to unite the nonpolar hydrogens added by SYBYL for the partial atomic charge calculation. The partial charges on the nonpolar hydrogens were added to that of the hydrogen-bearing carbon also in AUTOTORs.

In the analyses, 10 dockings were performed; in the analysis of the docked conformations, the clustering tolerance as different conformations for the rmsd was 1.0 Å. The step sizes were 0.2 Å for translations and 5° for orientations and torsions. The α and β parameters determined the size of the mutation in the genetic algorithms, LGA. The Cauchy distribution parameters were: $\alpha = 0$ and $\beta = 1$. Note that random changes were generated in the genetic algorithm by a Cauchy distribution.

In the LGA dockings, an initial population of random individuals with a population size of 50 individuals was used; a maximum number of 2.5×10^8 energy evaluations; a maximum number of generations of 2.7×10^4; an elitism value of 1, which was the number of top individuals that automatically survived into the next generation; a mutation rate of 0.02, which was the probability that a gene would undergo a random change; and a cross-over rate of 0.80, which was the probability that two individuals would undergo cross-over. Proportional selection was used, where the average of the worst energy was calculated over a window of the previous 10 generations. In the LGA dockings, the pseudoSolis and Wets local search method was used, having a maximum of 300 iterations per local search; the probability of performing local search on an individual in the population was 0.06; the maximum number of consecutive successes or failures before doubling or halving the local search step size, r, was 4, in both cases; and the lower bound on r, the termination criterion for the local search, was 0.01.

TCR/Peptide/MHC Complex Structure. To make the whole TCR/peptide/MHC complex structure, superposition was done between the docked structure of the TCR/peptide and the docked structure of peptide/HLA or between the docked structure of the TCR/peptide and the crystal structure of the peptide/HLA complex. Then, the peptide structure was removed from the system. The structures obtained were further energy-minimized (MOE software).

ACKNOWLEDGMENTS. We thank M. Karplus for technical advice and D. Keskin for helpful comments. This work was supported by National Institutes of Health Research Grant 5RO1 AI049524 and National Multiple Sclerosis Society Award RG3796A3.

1. Bjorkman PJ, *et al.* (1987) The foreign antigen binding site and T cell recognition regions of class I histocompatibility antigens. *Nature* 329:512–518.
2. Brown JH, Jardetzky TS, Gorga JC, Stern LJ, Urban RG (1993) Three-dimensional structure of the human class II histocompatibility antigen HLA-DR1. *Nature* 364:33–39.
3. Rudolph MG, Stanfield RL, Wilson IA (2006) How TCRs bind MHCs, peptides, and coreceptors. *Annu Rev Immunol* 24:419–466.
4. Hedrick SM, Cohen DI, Nielsen EA, Davis MM (1984) Isolation of cDNA clones encoding T cell-specific membrane-associated proteins. *Nature* 308:149–153.
5. Yanagi Y, *et al.* (1984) A human T cell-specific cDNA clone encodes a protein having extensive homology to immunoglobulin chains. *Nature* 308:145–149.
6. Bentley GA, Boulot G, Karjalainen K, Mariuzza RA (1995) Crystal structure of the beta chain of a T cell antigen receptor. *Science* 267:1984–1987.
7. Mak TW (2007) The T cell antigen receptor: "The Hunting of the Snark." *Eur J Immunol* 37(Suppl 1):S83–S93.
8. Garboczi DN, *et al.* (1996) Structure of the complex between human T-cell receptor, viral peptide and HLA-A2. *Nature* 384:134–141.
9. Garcia KC, *et al.* (1996) An alphabeta T cell receptor structure at 2.5 A and its orientation in the TCR-MHC complex. *Science* 274:209–219.
10. Hahn M, Nicholson MJ, Pyrdol J, Wucherpfennig KW (2005) Unconventional topology of self peptide–major histocompatibility complex binding by a human autoimmune T cell receptor. *Nat Immunol* 6:490–496.

11. Wucherpfennig KW, *et al.* (1994) Clonal expansion and persistence of human T cells specific for an immunodominant myelin basic protein peptide. *J Immunol* 152:5581–5592.
12. Wucherpfennig KW, *et al.* (1994) Structural requirements for binding of an immunodominant myelin basic protein peptide to DR2 isotypes and for its recognition by human T cell clones. *J Exp Med* 179:279–290.
13. Morris GM, Goodsell DS, Huey R, Olson AJ (1996) Distributed automated docking of flexible ligands to proteins: Parallel applications of AutoDock 2.4. *J Comput Aided Mol Des* 10:293–304.
14. Stoddard BL, Koshland DE, Jr (1992) Prediction of the structure of a receptor-protein complex using a binary docking method. *Nature* 358:774–776.
15. Maynard J, *et al.* (2005) Structure of an autoimmune T cell receptor complexed with class II peptide- MHC: Insights into MHC bias and antigen specificity. *Immunity* 22:81–92.
16. Li Y, *et al.* (2005) Structure of a human autoimmune TCR bound to a myelin basic protein self-peptide and a multiple sclerosis-associated MHC class II molecule. *EMBO J* 24:2968–2979.
17. Hausmann S, Martin M, Gauthier L, Wucherpfennig KW (1999) Structural features of autoreactive TCR that determine the degree of degeneracy in peptide recognition. *J Immunol* 162:338–344.
18. Wucherpfennig KW, Hafler DA, Strominger JL (1995) Structure of human T-cell receptors specific for an immunodominant myelin basic protein peptide: Positioning of T-cell receptors on HLA-DR2/peptide complexes. *Proc Natl Acad Sci USA* 92:8896–8900.
19. Fechteler T, Dengler U, Schomberg D (1995) Prediction of Protein Three-Dimensional Structures in Insertion and Deletion Regions: A Procedure for Searching Databases of Representative Protein Fragments Using Geometric Scoring Criteria. *J Mol Biol* 253:114–131.
20. Levitt M (1992) Accurate Modeling of Protein Conformation by Automatic Segment Matching. *J Mol Biol* 226:507–533.
21. Hennecke J, Carfi A, Wiley DC (2000) Structure of a covalently stabilized complex of a human $\alpha\beta$ T-cell receptor, influenza HA peptide and MHCII molecule, HLA-DR1. *EMBO J* 19:5611–5624.

doi: 10.1111/j.1365-2222.2007.02898.x

Clinical and Experimental Allergy, **38**, 405–412

ORIGINAL PAPER **Asthma and Rhinitis**

Seasonal changes in antigen-specific T-helper clone sizes in patients with Japanese cedar pollinosis: a 2-year study

S. Horiguchi*, Y. Tanaka†, T. Uchida*, H. Chazono*, T. Ookawa*, D. Sakurai* and Y. Okamoto*

**Department of Otolaryngology, Head and Neck Surgery, Graduate School of Medicine, Chiba University, Chiba, Japan and †Department of Immunology, Graduate School of Medicine, Chiba University, Chiba, Japan*

Clinical and Experimental Allergy

Summary

Background Allergic rhinitis (AR) is a typical type I allergic disease that occurs through the induction of allergen-specific effector T cells. Once established, new effector T cells derive mostly from memory T cells that are capable of surviving for extended periods, although the mechanisms by which these memory functions are maintained have not yet been clarified. In particular, the exact life-span of memory T cells is still not well understood.

Objective Pollinosis patients seemed to be suitable subjects to investigate because such patients are exposed to antigens strongly for only a limited period once a year. We compared the seasonal changes in memory T-helper type 2 (Th2) between pollinosis and perennial allergic subjects.

Methods The clone sizes of the Japanese cedar pollen-specific memory Th cells were measured by an ELISPOT assay using specific peptides from the patients with cedar pollinosis, and the seasonal changes were noted. This study was performed for 2 years. The cedar-specific IgE levels in the peripheral blood were also studied. Mite allergy patients were also enrolled in the study.

Results The Japanese cedar-specific IL-4-producing Th2 cells were detected in all patients examined, although the number of cells was low. These Th memory cells increased during the pollen season and decreased during the off-season. However, more than 60% of the cedar-specific memory Th2 cells survived up to 8 months after the pollen season. The cedar-specific IgE levels exhibited changes similar to the cedar-specific Th cells. On the other hand, there was no drifting of Th memory clone size with the mite allergics, and the IgE levels also did not change.

Conclusions While pollen-specific Th cells decreased after pollen exposure, their memory functions continued. Memory clone size maintenance therefore requires repetitive antigen irritation.

Correspondence:
Shigetoshi Horiguchi, Department of Otolaryngology, Head and Neck Surgery, Graduate School of Medicine, Chiba University, 1-8-1 Inohana, Chuo-ku, Chiba 260-8670, Japan.
E-mail: horiguti@faculty.chiba-u.jp

Keywords allergic rhinitis, clone size, IgE, memory T cell, Th2
Submitted 25 January 2007; revised 6 September 2007; accepted 16 October 2007

Introduction

In recent years, many countries have experienced an increase in the prevalence of allergic rhinitis (AR) [1, 2]. In Japan, Japanese cedar (*Cryptometria japonica*) and Japanese cypress (*Chamaecyparis obtusa*) pollens are considered to be the major unique allergens and their extent of dispersal is quite large, travelling more than 100 km and thus causing serious pollinosis [3, 4].

Pollinosis is thought to be an adaptive immune response that manifests as a type I allergic reaction, and it occurs as a consequence of fundamental allergenic mechanisms involving the induction of pollen-specific T-helper type 2 (Th2) effector cells from naïve Th0 cells [5]. Most effector T cells are short-lived, but few effector T cells become long-lived memory T cells. Once a memory T cell is established, it retards the induction of new effector T cells from naïve Th0 cells, according to the principle of the 'original antigenic sin'. Hence, most effector T cells are derived from memory T cells [6–10]. This concept describes a phenomenon in which the antibody response elicited in an individual after a secondary viral infection reacts more strongly to the viral variant that originally infected the individual. A similar phenomenon

is likely to be observed in Th cell responses as they play critical roles in promoting antibody responses.

Patients with type I allergy are thought to have allergen-specific memory Th cell clones. Immune-therapeutic intervention directed at diminishing the size of these clone memory Th2 cells and shifting the cytokine type of memory Th clones is thought to play a considerably important role in finding a complete cure.

However, the mechanism by which the antigen-specific Th memory clone is maintained in an allergic patient has not yet been clarified. There are several reports describing the peripheral blood to be re-stimulated by a specific antigen, while the Th2 cytokine response was measured both in season or/and out of season [11–13] as well as before and after immunotherapy [14–16]. In those studies, peripheral blood mononuclear cells (PBMCs) were stimulated by an antigen, and measured Th2 cytokine or its mRNA. However, those cytokine responses that were re-stimulated by whole antigen reflected various kinds of cells such as T cells, B cells, macrophages and antigen-presenting cells and did not precisely reflect the function or the exact number of antigen-specific Th cells. Because the Th cell response is restricted in major hitocompatibility complex class II, it is necessary to use the Th cell epitope of class II restrictive to measure the reaction only for Th cell clones respond to allergen. Our purpose is to estimate the duration of life-span of allergen-specific memory T cells. We therefore directly examined the number of specific Th2 cells to respond to class II restrictive T cell epitope, which matched with Japanese human leukocyte antigen (HLA) variation. These kinds of studies have not yet been carried out. Pollinosis seemed to be a suitable subject to investigate the life-span of Th memory clones because patients are exposed to the antigen for only a limited period. In the present study, we examined the specific memory clone size, which is a population size of memory T cells that recognizes the same specific HLA restrictive epitope and produces isologous cytokine. We tried to detect IL-4 productive cells using only seven T cell epitopes; as a result, the total summation of these seven kinds of clones is the clonal size.

The limited seasonal nature of antigen exposure is useful for elucidating the mechanisms used in the maintenance of Th memory clone sizes. We examined the Japanese cedar pollen-specific Th clone sizes and the associated seasonal changes in patients with cedar pollinosis, while also comparing the yearly change in the clone size due to pollinosis with that due to perennial mite allergies that were detected by 14 T cell epitopes.

Materials and methods

A total of 41 patients with Japanese cedar pollinosis were enrolled in this study. The ages of the 20 males and 21 females ranged from 20 to 51, with an average of 31.1 years. The diagnosis of Japanese cedar pollinosis was based on the occurrence of typical nasal symptoms during the cedar pollen season and the detection of Japanese cedar-specific IgE by CAP-RAST (score: 2 or more). All patients had symptoms for at least 3 years. None of the patients received immunotherapy or immunosuppressive drugs (including steroids) within 8 weeks before the start of the study. The study received prior approval from the Ethics Committee of the Chiba University (Chiba, Japan). A written, witnessed informed consent was obtained from all patients. The study design is shown in Table 1. From 2003 to 2004, 23 patients participated in this study, and from 2004 to 2005, another 18 patients were enrolled. Twenty-two patients with perennial AR due to mite were also enrolled in this study. The ages of the 10 males and 11 females with perennial AR were from 20 to 48, with an average of 28.8 years. The diagnosis of mite allergy was based on the occurrence of typical nasal symptoms and the detection of Der f IgE by CAP-RAST (score: 2 or more).

Ten healthy subjects were also enrolled as controls. They were all negative for symptom episodes and allergen IgE.

The blood samples were collected every 3 months after July, and the PBMCs were obtained by the Ficoll–Hypaque method from the patients. The samples were stored in liquid nitrogen until analysis.

Clinical symptoms

The nasal symptoms were evaluated on a scale from 0 to 4 in accordance with the practical guidelines for the treatment of AR [17], as follows: 0, no sensation; 1, mild; 2, moderate; 3, severe; and 4, extremely severe. Daily episodes of sneezing and nose blowing were rated 0 to 4, as follows: 0, none; 1, 1–5 episodes; 2, 6–10 episodes; 3, 11–20 episodes; and 4, >20 episodes. The medication was also recorded according to drug characteristics and duration of usage, according to the guidelines, as follows: antihistamine, mast cell stabilizers and vasoconstrictor were 1, and topical ocular or nasal steroids were 2.

Reagents

Antibodies. The monoclonal antibodies (MoAb) used for the ELISPOT assay were acquired from MABTECH (Stockholm, Sweden). For coating, MoAb 82-4 and MoAb 1-DIK were used to coat human IL-4 and IFN-γ, respectively. For detection, MoAb 12-1 and 7B6-1 were used to detect human IL-4 and IFN-γ, respectively. For the FACS analysis, anti-human Cy5-conjugated CD4, FITC-conjugated IFN-γ and PE-conjugated IL-4 were purchased from Dako (Tokyo, Japan).

Peptides. A recombinant hybrid peptide was used for the ELISPOT assay. This peptide comprised of the seven CD4 T

Table 1. Time schedule for examination

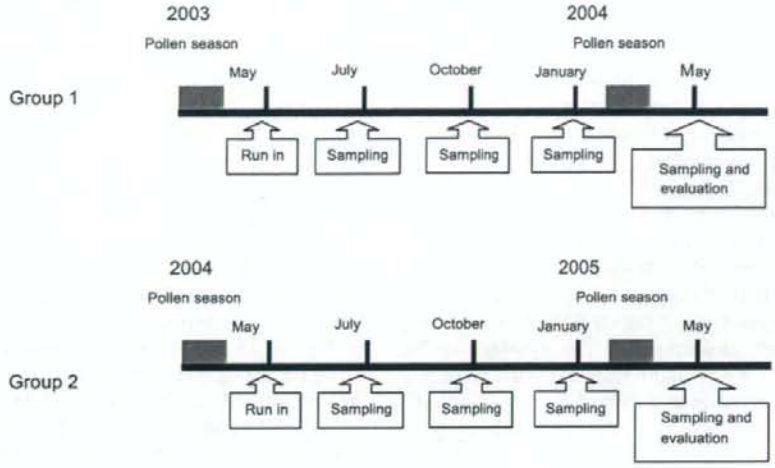

The Group 1 patients were recruited after the pollen season of 2003 and the Group 2 patients were recruited after pollen season of 2004. The blood sampling was performed every 3 months starting in July. The last blood sampling was performed after the pollen season of May, and the samples were analysed simultaneously.

cell determinants of Cry j 1 and Cry j 2, and the major Japanese cedar pollen allergens. Almost all the patient populations responded to this hybrid peptide, which is comparable to the response to Cry j 1 and Cry j 2. Moreover, because the seven peptides do not contain IgE-binding residues of *C. japonica* allergens, the recombinant peptide will not directly influence IgE-bearing cells such as mast cells, basophils and B cells [18]. The recombinant peptides for mite allergy were also prepared. This peptide comprised of the 14 CD4 T cell determinants of Der f 1 [19] and Der f 2 [20], and the major mite allergens. Almost all the patient populations responded to these peptides, which is comparable to the response to Der f 1 and Der f 2. Those peptides were Class II restricted and recognized Th cells only.

ELISPOT

The ELISPOT assay was performed according to the manufacturer's instructions. Briefly, the anti-human IL-4 or IFN-γ MoAbs were diluted to a concentration of 15 μg/mL in sterile, filtered (0.45 μm) PBS (pH 7.2), and 100 μL/well was added onto nitro-cellulose plates (Millititre, Millipore Corp., Bedford, MA, USA). The plates were incubated overnight at 4 °C and the unbound antibodies were washed with filtered PBS thereafter. After the last wash, the PBS was sucked through the membrane under vacuum (Millipore Corp.). One hundred microlitres of the pre-stimulated cell suspension was added to each well in duplicate, and the plates were incubated for 10 h at 37 °C. The cells were subsequently washed before adding 100 μL of the biotinylated MoAbs (1 μg/mL), and were then incubated for 2 h at room temperature. The plates were then washed and incubated for 90 min at room temperature with 100 μL of streptavidin alkaline phosphatase (Mabtech, Stockholm, Sweden) at a dilution of 1 : 1000. The unbound conjugate was removed by another series of rinsing before 100 μL of BCIP/NBT substrate solution (Bio-Rad, Richmond, CA, USA) was added, and the plates were incubated at room temperature until dark spots emerged (1 h). The colour development was stopped by repeated rinsing with tap water. After drying, the spots were captured photo-electrically and counted by a computed analysis to avoid any visual bias, using Auto Counter (ImmunoScan, CTL, Gmünd, Germany).

Pollen counts

The combined annual cedar and cypress pollen counts were measured using Durham pollen samplers.

Statistical analysis

Wilcoxon's paired rank sum tests were used to compare the mean values. A Friedman two-way ANOVA was used to

analyse paired data. Peason's tests were used to determine the correlation coefficients.

Results

The cedar and cypress pollen counts determined using the Durham samplers were 470 cm/season in 2004, which was 1/20 of the average for the last 10 years. In 2005, we obtained 7852 cm/season, which was threefold higher than that of the average for the last 10 years. The seasonal symptoms were comparatively mild in 2004, and comparatively serious in 2005. The mean symptom-medication scores during the pollen season in 2004 and 2005 were 1.4 ± 2.1 and 2.8 ± 2.3 (mean $\pm$ SD), respectively.

Before the study, we compared the peptide-specific Th2 clone size of the patients with that of healthy controls in October, which is off pollen season. After stimulation with 10 nmol/L of cedar-specific peptides, the mean values of the IL-4 spot from the healthy controls and patients with cedar pollinosis that were obtained are shown in Fig. 1. Positive spots were obtained only in the samples from the pollinosis patients, but not from controls (A), although spots were equally obtained in the samples from both patients and controls when stimulated by Con A as a pan T cell stimulant (B). We also confirmed peptides for mite. The IL-4 spots were obtained only in the samples from the patients, but not from the controls (Fig. 2a), although spots were equally obtained in the samples from both patients and controls when stimulated by Con A as a pan T cell stimulant (Fig. 2b). Peptide-specific IL-4 spots were detected in all samples examined. Approximately 10–100 peptide-specific IL-4 spots were observed in the wells

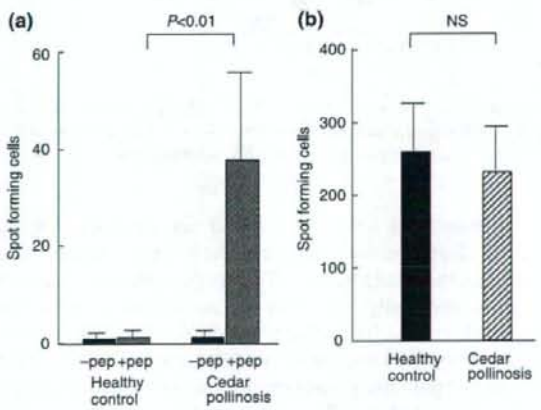

Fig. 1. The mean values of IL-4 spots in the samples from the healthy control subjects and patients with cedar pollinosis are shown. (a) 1×10^5 cells were stimulated by a peptide derived from Cry j 1 and Cry j 2. The spots were obtained only in the samples from the pollinosis patients, but not from the controls. (b) 1×10^4 cells were stimulated by Con A, a pan T cell stimulant. The spots were equally obtained in the samples from both the patients and the controls. NS, not significant.

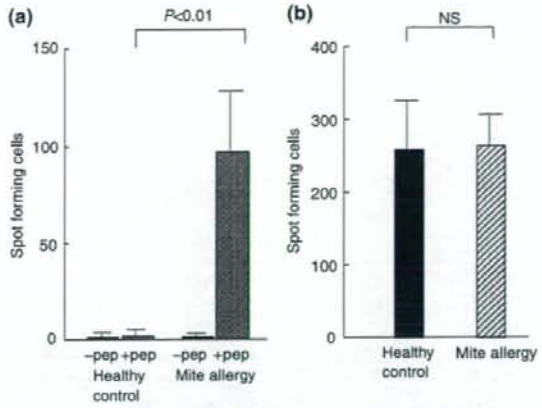

Fig. 2. The mean values of IL-4 spots in the samples from the healthy control subjects and patients with cedar pollinosis are shown. (a) 1×10^5 cells were stimulated by a peptide derived from Der f 1 and Der f 2. The spots were obtained only in the samples from the pollinosis patients, but not from the controls. (b) 1×10^4 cells were stimulated by Con A, a pan T cell stimulant. The spots were equally obtained in the samples from both the patients and the controls. NS, not significant.

incubated with 10^5 PBMC based on the ELISPOT assay. These spots were analysed in triplicate in each of the experiments and exhibited good reproducibility.

We carried out a depletion assay in advance with whole PBMC from three patients with Japanese cedar pollinosis using an antibody-conjugate magnetic bead kit (MACS system, Miltenyi Biotec GmbH, Tokyo, Japan). When CD4 was depleted, the spots of ELISPOT disappeared; however, after the depletion of CD8, the number of spots was equal to that with whole PBMC. The depletion of CD28 also caused the spots to disappear. These results show that the present ELISPOT assay using a hybrid peptide was CD4 restricted and the CD28 expression was indispensable for the detection of the spots (data not shown).

The seasonal changes in peptide-specific IL-4 spots are shown in Fig. 3. The IL-4 spots decreased after July, and were at their lowest in January before the onset of the cedar pollen season, which were almost 60% of those observed in July. The IL-4 spots increased during the cedar pollen season in 2004 despite the small amount of pollen (Fig. 3a). The same trend in seasonal changes was obtained during the 2005 season. The IL-4 spots decreased after July, and were at their lowest in January before the onset of the cedar pollen season, which were almost 60% of those observed in July (Fig. 3b). Interestingly, the clone size on May 2005 was 40% larger than that on July 2004. This phenomenon was not seen during the 2004 season.

The seasonal changes in the cedar-specific IgE levels in the serum of the patients are shown in Fig. 4. While the cedar-specific IgE decreased after the pollen season in 2003, it did not increase during the cedar pollen season in